

Photochemical Production of NADH Using Cobaloxime Catalysts and Visible-Light Energy

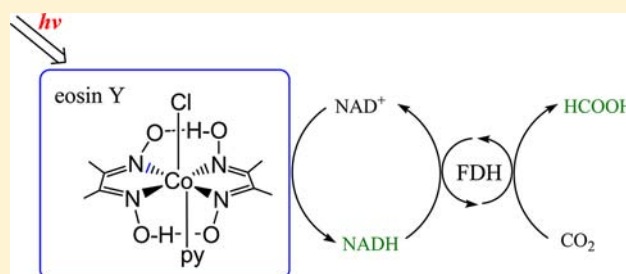
Jin Ah Kim,[†] Soojin Kim,[†] Jungha Lee,[†] Jin-Oog Baeg,[‡] and Jinheung Kim^{*,†}

[†]Department of Chemistry and Nano Science, Ewha Womans University, Seoul 120-750, Korea

[‡]Advanced Chemical Technology Division, Korea Research Institute of Chemical Technology (KRICT), Daejeon 305-343, Korea

Supporting Information

ABSTRACT: In this study, a visible-light-driven photocatalytic system for the generation of dihydronicotinamide adenine dinucleotide (NADH) from aqueous protons was examined using cobaloxime as a catalyst, eosin as a photosensitizer, and triethanolamine as a sacrificial electron donor. Irradiation of a reaction solution containing cobaloxime, eosin, and triethanolamine (TEOA) converted NAD^+ to NADH with a yield of 36% in a phosphate buffer. The reaction rates for the production of NADH were dependent on the concentrations of the catalyst, NAD^+ , and TEOA. Introduction of an electron-donating or -withdrawing substituent in the para position of the pyridine changed the rate constant and affected the conversion efficiency. The rates obtained by the different substituents were linearly correlated with the Hammett coefficients of the introduced substituents. Last, reduction of CO_2 was carried out in the presence of formate dehydrogenase using NADH photochemically generated using the cobaloxime/eosin/TEOA system.



INTRODUCTION

Because of the recent significant concern regarding the fast depletion of fossil fuels, the most important challenges are the development of alternative energy supplies. One of the most important goals for achieving long-term storage of renewable energy is to find effective systems yielding chemical energy in the form of a reducing potential, such as dihydronicotinamide adenine dinucleotide (NADH), nicotinamide adenine dinucleotide phosphate (NADPH), etc., using solar energy. NADH/NADPH, which is ubiquitous in all living systems by serving as biological electron transporters, can be used to carry out valuable reactions through related enzymes and catalysts, such as conversion of CO_2 to hydrocarbon fuels, production of H_2 from aqueous protons, etc.^{1–5} The conversion of less than 5% of solar energy has been shown to be sufficient to supply the annual worldwide energy needs. Therefore, the photocatalytic regeneration of NADH from aqueous protons has attracted significant scientific interest because of its close relevance to solar energy conversion and artificial photosynthesis. The enzymatic methods for regeneration of NAD(P)H have been well established and involve formate dehydrogenase (FDH), alcohol dehydrogenase, and ferridoxin-NADP reductase.^{6–9} As synthetic catalysts, a couple of systems employing heavy transition metals, such as ruthenium, rhodium, and iridium, have been developed for the electrochemical and/or photochemical regeneration of NADH.^{10–15} The organometallic rhodium complex $[(\text{cyclopentadienyl})\text{Rh}(\text{bipyridyl})(\text{H}_2\text{O})]^{2+}$ has been frequently used in studies of NADH regeneration because of its relatively good reactivity and selectivity but is still far from being used in practical applications because of its

reactivity and high cost. Therefore, developing more efficient photocatalytic systems utilizing cheap and earth-abundant metals is of considerable current interest. To the best of our knowledge, no catalyst based on a low transition metal has been reported for the photocatalytic regeneration of NADH.

Since Connolly and Espenson reported the reduction of protons to H_2 using a cobaloxime system, $\text{Co}^{\text{II}}(\text{dmgBF}_2)_2(\text{H}_2\text{O})_2$ [$\text{dmgBF}_2 = (\text{difluoroboryl})\text{-dimethylglyoxime}$],¹⁶ various research groups have exerted great efforts to develop an efficient system to generate H_2 using molecular cobalt catalysts.^{17–28} Among these cobalt catalysts, $[\text{Co}(\text{dmgH})_2\text{pyCl}]$ ($\text{dmgH} = \text{dimethylglyoximate}$; $\text{py} = \text{pyridine}$) has been studied for the electrochemical and photochemical production of H_2 .^{22–29} In their proposed mechanism, a cobalt(I) intermediate generated by electron transfer from the photoexcited chromophore was coupled with a proton to produce cobalt(III) hydride species, which are believed to be responsible for the formation of H_2 . On the basis of these findings, we were interested in the formation of a metal hydride intermediate from photoreaction with the cobalt catalysts because a hydride-transfer reaction is also expected to reduce NAD^+ . We recently developed a simple system for the photocatalytic production of NADH using platinum nanoparticles acting as both a photosensitizer and a catalyst.²⁹ In our continuous efforts to develop less expensive photocatalytic systems for NADH regeneration, here, we report for the first time the use of three cobaloxime complexes in a visible-

Received: January 24, 2012

Published: July 26, 2012

light-driven photocatalytic system for NADH regeneration from aqueous protons in the presence of eosin Y as a photosensitizer. The system containing the cobalt catalyst was found to be effective in the photogeneration of the enzymatically active NADH and could also convert CO₂ to formic acid in the presence of FDH.

EXPERIMENTAL SECTION

Materials and Instrumentation. Water was purified using a Milli-Q purification system. All reagents purchased from Aldrich were used without further purification. Formate dehydrogenase (FDH) was purchased from Sigma-Aldrich. [Co(dmgh)₂pyCl] (1), [Co(dmgh)₂(py-NMe₂)Cl] (2), and [Co(dmgh)₂(py-COOMe)Cl] (3) [py = pyridine; py-NMe₂ = 4-(dimethylamino)pyridine; py-COOMe = methyl isonicotinate] were prepared according to previously published methods.²¹

UV-vis spectra were recorded on a Hewlett-Packard 8453 spectrophotometer. Emission spectra were collected on a Perkin-Elmer LS 55 luminescence spectrophotometer.

Photocatalytic NADH Production. The typical photochemical generation of NADH by cobaloxime and eosin Y was carried out in the presence of NAD⁺ and triethanolamine (TEOA) in a phosphate buffer (pH 5.0–9.0) at 25 °C. Photoreactions were performed in a 3 mL glass cuvette (vial) equipped with a small magnetic stirrer and a stopper. Samples (a total volume of 1 mL) consisting of all of the components were transferred into the cuvettes and then illuminated. Deaerated samples were prepared by repeated evacuation followed by argon flushing. Photolysis was performed using a 330 W arc xenon lamp equipped with a water filter and a 420 nm cutoff filter. The production of NADH was determined by UV absorption at 340 nm ($\epsilon = 6220 \text{ cm}^{-1} \text{ M}^{-1}$). Data points were obtained from the average of three independent measurements. The rates of [NADH] per hour determined from the slope of linear plots of [NADH] versus time increased linearly with the concentration of 1, NAD⁺, or TEOA.

The photoproduct NADH was also characterized by high-performance liquid chromatography (HPLC; Youngin Instrument, Korea, Acme 9000) using an Inertsil C18 column (ODS-3 V, 4.6 i.d. \times 150 mm) and confirmed with NADH (purchased from Aldrich). The HPLC conditions were as follows: the mobile phase was 0.085% phosphoric acid; the flowing rate was 1.0 mL min⁻¹; the monitor wavelength was 210 nm; the retention times of NAD⁺ and NADH were 18.8 and 18.1 min, respectively.

Measurement of the Quantum Yield. All procedures except photolysis were performed under red light. The photon flux was measured at the same distance as the photoreaction described above using the Reference Solar Cell and Meter (Newport, model 91150, 2 \times 2 cm calibrated with KG2 window). The quantum efficiency of NADH production with a solution of 0.13 mM 1/0.1 mM eosin Y/0.5 mM NAD⁺/0.2 M TEOA was evaluated by illuminating a 20 nm bandpass filter at 420 nm for 2 h. The quantum yield (Φ_{H}) was defined according to the following formula:

$$\Phi_{\text{H}} = 2(\text{moles of NADH})/\text{moles of incident photon}$$

H₂ Evolution. The photolysis was carried out for a 1 mL solution sealed in a vial with silicone/poly(tetrafluoroethylene) septa. Samples typically contained 0.13 mM 1, 0.1 mM eosin, and 0.20 M TEOA with and without 0.5 mM NAD⁺ in a phosphate buffer solution (pH 7.0). Sample vials were deoxygenated by bubbling nitrogen through them for 15 min. Part of the gas above the solution was collected by a gastight syringe and injected onto a gas chromatograph (DS GC-6200, Seoul, Korea) equipped with a thermal conductivity detector and a carbosphere column (Alltech 8011/2, USA; column temperature, 60 °C; argon as the carrier gas).

Reduction of CO₂. The conversion of CO₂ was performed with fresh solutions containing the above NADH photogeneration system and FDH (20 units) prepared before each experiment. The solutions were bubbled with argon to remove O₂ and saturated with CO₂ before irradiation. Formic acid was analyzed and quantitated by HPLC (Youngin, Korea, model YL9100) using a column (Inertsil ODS-3 V, 5

μm , 4.6 \times 150 mm) and a 0.01% phosphoric acid solution as the eluent.

RESULTS AND DISCUSSION

A series of cobaloxime complexes, 1–3, were prepared as reported^{21,25,30} and evaluated as molecular catalysts for the photoproduction of NADH (Figure 1).

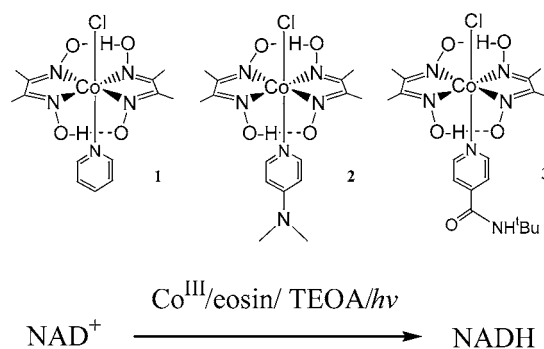


Figure 1. Chemical structures of cobalt complexes 1–3 and the photoreaction of NADH formation.

A series of experiments using complexes 1–3 for NADH production were carried out by employing visible-light irradiation (a 420 nm cutoff filter) under nitrogen. The formation of 1,4-NADH was followed by monitoring of the absorbance at 340 nm. When the photocatalytic reaction system contained 1, eosin (EY²⁻), and triethanolamine (TEOA) as a sacrificial electron donor in the presence of NAD⁺ in a phosphate buffer (pH 7.0), the conversion yield of NAD⁺ turned out to be around 24 and 36% after 4 and 9 h of irradiation, respectively (Table 1, runs 1 and 3, and Figure S1 in

Table 1. Photocatalytic Reduction of NAD⁺ with 1–3 and Eosin^a

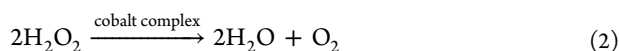
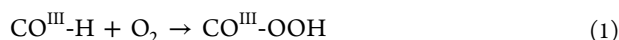
run	catalyst	time (h)	NADH yield (%) ^b	initial rate ($\mu\text{M h}^{-1}$) ^c
1	1	4	24 \pm 2	30 \pm 2
2	1	4	11 \pm 4	14 \pm 3
3	1	9	36 \pm 3	
4	2	4	29 \pm 2	37 \pm 2
5	2	9	29 \pm 4	
6	3	4	23 \pm 2	28 \pm 2
7	3	9	25 \pm 2	

^aStandard conditions for visible-light-driven NADH production experiments: 1–3 (0.13 mM), eosin (0.10 mM), NAD⁺ (0.50 mM), TEOA (0.20 M) in a phosphate buffer (0.15 M) at pH 7.0 and room temperature under nitrogen. In run 2 only, the reaction was performed under air. ^bThe yield was calculated based on [NAD⁺]. ^cInitial rates are for NADH photoproduction.

the Supporting Information). No NADH was detected in the absence of 1, indicating that the cobalt complex was a key component of the NADH production system. In the absence of eosin and/or TEOA, only trace amounts of NADH were observed under the same conditions. The quantum yield for photogeneration of NADH was determined by measuring the net yield of the two-electron process associated with the reduction of one NAD⁺ molecule (see the Experimental Section). A quantum yield of 0.044 was obtained by illuminating the solution of 1/NAD⁺/eosin Y/TEOA for 2 h,

which was similar to that determined for H₂ photoproduction for the eosin system.²⁵

Molecular O₂ was reported to readily react with a chemically or electrochemically reduced rhodium(III) hydride intermediate for NADH regeneration.^{31,32} However, in many reports on the photoproduction of H₂ with cobalt catalysts, the O₂ effect has never been studied because of the need to produce and detect H₂ under anaerobic conditions. Thus, we decided to examine the effect of O₂ on the photoreduction of NAD⁺ with **1**. In the aerobic and anaerobic photoreactions with **1**, the formation rate of NADH under nitrogen was determined to be faster (30 μM h⁻¹ under nitrogen versus 14 μM h⁻¹ under air), indicating that the photoreaction was sensitive to O₂ (Table 1, run 2, and Figure S2 in the Supporting Information). Upon visible-light irradiation of the related cobalt complexes, evidence for the formation of the cobalt(III) hydride intermediate was proposed, and some evidence for the presence of such an intermediate was reported based on absorption and electrochemical data.^{17,23,24,26,27} The cobalt(III) hydride species generated during the photoreaction may have an affinity toward O₂ for the generation of a Co^{III}OOH species (eq 1). The formation of such Co^{III}OOH intermediates has often been reported in aqueous systems.^{33,34} However, the potential release of H₂O₂ from Co^{III}OOH was not detected after irradiation for 4 h based on the iodide test. We then examined the possible photodecomposition of H₂O₂ in the presence of **1** and TEOA. When H₂O₂ (0.2 mM) was irradiated in the presence of **1** and TEOA for 1 h, no H₂O₂ was also observed in the final solution. It was reported that cobalt complexes could perform such a fast catalytic decomposition of H₂O₂ (eq 2).^{35,36} Our results confirm that the photochemical generation rate of NADH was influenced by molecular O₂. It has also been reported that the slower rate of the electrochemical NADH generation by a rhodium catalyst under air resulted from consumption of the rhodium(III) hydride species by O₂.^{31,32} On the basis of these observations, all of the following photoreactions were carried out under nitrogen.



In order to examine the effect of the nucleophilicity of the cobalt center, we compared the catalytic activity of **1** to **2** and **3**, which contain the electron-donating dimethylamino and electron-withdrawing *N-tert*-butylamido substituents in the para position of the axial pyridine, respectively. Introduction of the electron-donating substituent resulted in a higher rate, but the electron-withdrawing substituent caused a slight decrease in the rate (Table 1, runs 1, 4, and 6). This effect was plotted as log(*k*) versus the Hammett coefficients, which reflects the electronic properties of the substituents (Figure 2). The positive slope in the linear free enthalpy of activation correlation was in accordance with a nucleophilic attack of the cobalt(III) hydride species toward NAD⁺. Similar electronic properties in the rate constants for H₂ photogeneration were also reported with cobalt catalysts.²¹

The effect of the solution pH on the rate of NADH formation with **1** was also investigated. Figure 3 shows the time traces of NADH produced as the pH of the phosphate buffer solution was varied. At pH 7.0, the maximum rate of NADH generation was observed, while the lowest rate was observed at 9.0 after 4 h of irradiation. The rates at pH 5.0 and 6.0 were

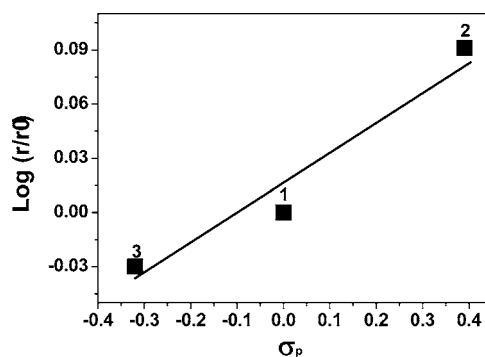


Figure 2. Linear correlation between the relative rates [$\log(r/r_0)$] of 1–3 and the Hammett coefficients of the para substituent of the axial pyridine in the cobalt catalysts. The initial rate of NADH formation using **1** corresponds to r_0 , and r indicates that using **2** or **3**. The rates were obtained from the time dependence of NADH production under steady-state irradiation of a phosphate buffer solution (pH 7.0) containing the cobalt complex (1–3, 0.13 mM), 0.10 mM eosin Y, 0.50 mM NAD⁺, and 0.20 M TEOA.

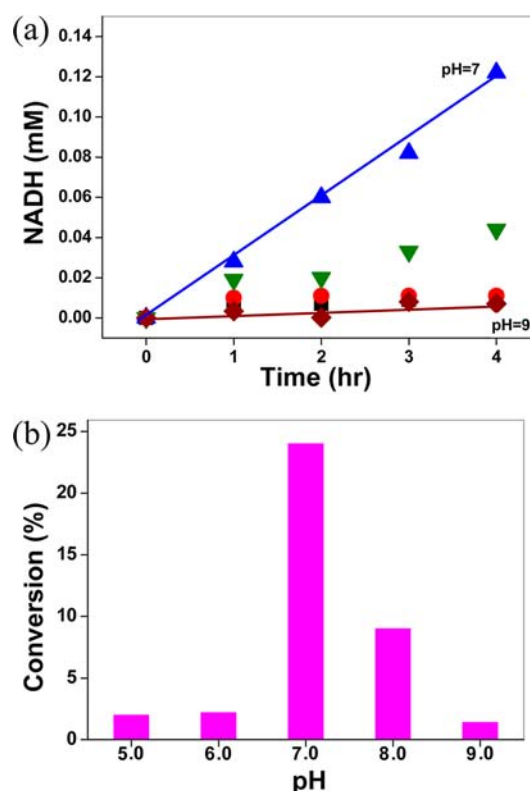


Figure 3. (a) Time traces of pH-dependent photocatalytic NADH production with **1** (0.13 mM), NAD⁺ (0.50 mM), eosin Y (0.10 mM), and TEOA (0.20 M) in 0.15 M phosphate buffer at 25 °C: pH 5 (red circles), 6 (black squares), 7 (blue triangles), 8 (green triangles), and 9 (brown diamonds). (b) Effect of the pH on NADH regeneration after 4 h of photoirradiation. The conversion yields were calculated based on the initial NAD⁺ concentration.

similar but much lower than that at pH 7.0, demonstrating that NADH generation was prominently inhibited at low proton concentrations. A decrease in the rate of NADH formation at acidic pH was shown to be due to the protonation of TEOA, which results in a less effective electron donor. The low reactivities at high pH may be due to the photochemical

decomposition of eosin by debromination, which has been suggested in other studies.²³

In order to examine the possible production of H₂ in the process of NADH formation, H₂ was analyzed under our reaction conditions because Eisenberg and co-workers demonstrated effective H₂ generation using the same catalytic system without NAD⁺.^{23,26} In the absence of NAD⁺, H₂ production corresponded overall to 15 turnovers of eosin at 5 h in a phosphate buffer (Figure 4). Compared to the previous report

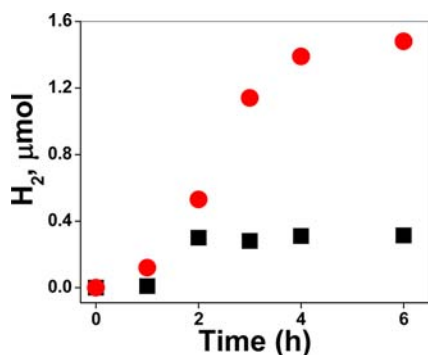
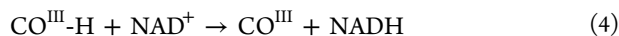
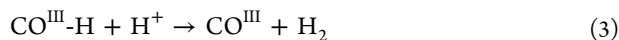


Figure 4. Visible-light-driven H₂ production in the absence (red circles) and presence (black squares) of 0.50 mM NAD⁺ in a phosphate buffer solution (pH 7.0). The reaction conditions were 0.13 mM **1**, 0.10 mM eosin Y, and 0.20 M TEOA.

carried out in CH₃CN/H₂O by Eisenberg and co-workers,^{23,26} the total yield of H₂ was relatively quite low because of the different reaction conditions. Interestingly, in the presence of NAD⁺, H₂ production was drastically reduced to afford the yield corresponding to 3 turnovers of eosin at 5 h, indicating that the reaction pathway for NADH formation (eq 4) significantly prohibited H₂ production. Upon 4 h of irradiation, the reduction in H₂ production in the presence of NAD⁺ was about 1.2 μmol, which was 10 times higher than the amount of NADH produced (24%, 0.12 μmol; Table 1). To understand the big difference between the amount of H₂ and NADH obtained under two different reaction conditions of the absence and presence of NAD⁺ upon 4 h of reaction, a possible decomposition pathway of NADH produced in the photoreaction was examined using **1**/eosin Y/TEOA. Indeed, NADH (1 mM) decomposed to NAD⁺ upon 4 h of irradiation (Figure S3 in the Supporting Information), and H₂ (32% based on the initial NADH) was observed as another reaction product (eq 5). The fact that some amount of H₂ was still observed in the above photoreaction performed even in the presence of NAD⁺ should be related to such a reaction pathway of NADH decomposition. The visible-light-driven photooxidation of NADH using platinum nanoparticles and an organic photosensitizer was reported and H₂ production also observed.² The presence of such reaction pathways of the oxidation of NADH and H₂ production should result in the low yield of NADH in the reduction of NAD⁺ with this system.



NADH production was dominant in the early stage of the photoreaction, then H₂ production derived from the oxidation

of NADH started, and finally the formation and decomposition of NADH stopped because of bleaching of the photolysis solution at about 5 h (Figure 4). The termination of H₂ evolution by **1** and eosin was also proposed as bleaching of the photolysis solution.²³ The amount of H₂ produced in the presence of NAD⁺ derived from the repeated formation and decomposition of NADH before bleaching. In a control experiment, when the bleached solution of **1** and eosin after 4 h of photoreaction was treated with additional NADH (1 mM), the production of H₂ by the mixture was negligible upon irradiation. These results indicate that the decomposed products of **1** and eosin somehow had no significant activity to produce H₂ using NADH.

The reaction rate of NADH photoproduction was found to depend on the concentration of the catalyst **1** (Figure 5a). As

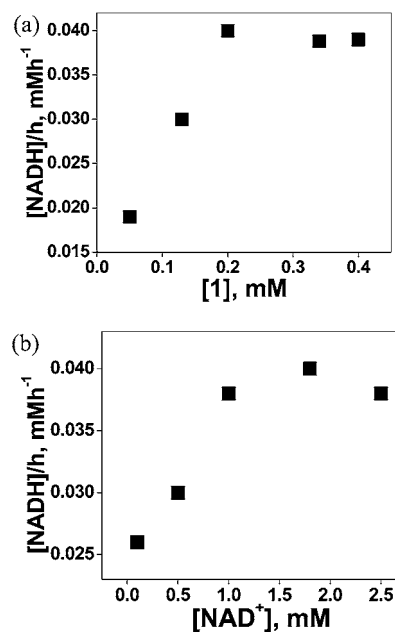


Figure 5. Dependence of NADH production rates as a function of (a) [**1**] and (b) [NAD⁺] in a phosphate buffer containing TEOA at 25 °C under nitrogen. The other components were (a) 0.50 mM NAD⁺, 0.10 mM eosin Y, and 0.20 M TEOA and (b) 0.13 mM **1**, 0.10 mM eosin, and 0.20 M TEOA.

the amount of **1** increased from 0.05 to 0.32 mM, the rate of NADH formation increased. The final conversion yield obtained after irradiation for 4 h also increased from 15 to 33% based on the concentration of NAD⁺. However, further increases in the cobalt concentration above 0.32 mM led to a constant rate of NADH production, implying that the photon flux for the photochemical NADH generation became turnover-limiting at these concentrations of **1**. The rate-limiting photon flux for H₂ production with **1** was also observed by Alberto and co-workers.³⁷

Studies on the effect of the NAD⁺ concentration were also carried out. The results shown in Figure 5b demonstrate that the photochemical reaction had a higher rate of NADH production when the concentration of NAD⁺ was increased. At 0.13 mM **1** and 50 mM TEOA, the NADH production rate was also saturated at 1.0 mM NAD⁺, also related to the rate limiting of the photon flux.

To obtain further insight into the reaction mechanism of NADH generation, we examined the effect of the TEOA

concentration. As the concentration of TEOA was increased to 0.2 M, the rate increased to $38 \mu\text{M h}^{-1}$ and the conversion yield ranged from 11 to 30% after 4 h of irradiation (Figure 6a). The

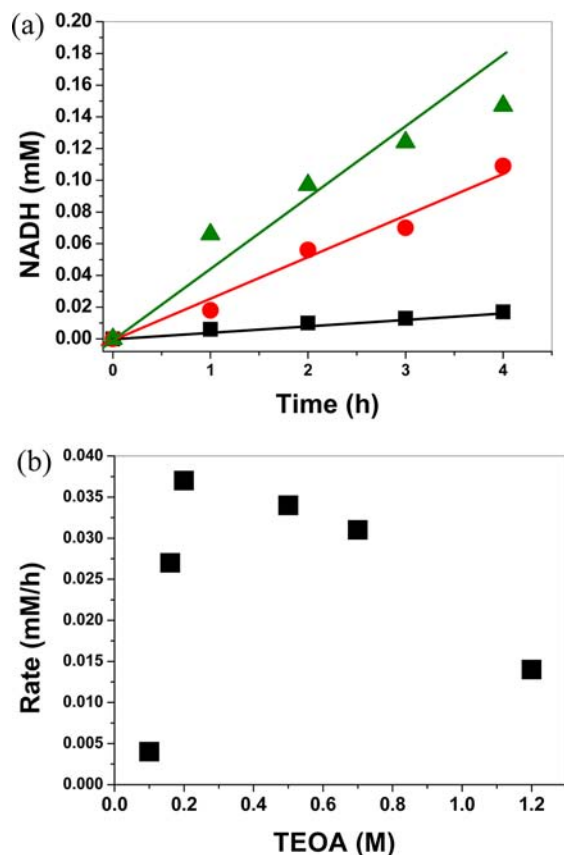


Figure 6. (a) Time dependence of NADH production with varying amounts of TEOA in a phosphate buffer solution (pH 7.0). Concentrations of TEOA: 0.10 (black squares), 0.16 (red circles), and 0.20 M (green triangles). The concentrations of the other components were 0.13 mM **1**, 0.10 mM eosin Y, and 0.50 mM NAD^+ . (b) Dependence of the NADH production rate on the concentration of TEOA.

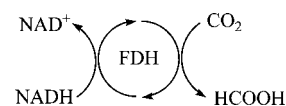
rate then clearly started to decrease after 0.5 M TEOA (Figures 6b and S4 in the Supporting Information). Scavenging EY^{2-*} by TEOA would retard the formation of the cobalt(I) species, which was an intermediate in the formation of a cobalt hydride species. To better understand the interaction between eosin and TEOA, quenching experiments of EY^{2-*} with TEOA were performed using fluorescence measurements. The reductive quenching process followed the Stern–Volmer behavior, with the quenching rate constant (k_q) value being $13 \pm 0.5 \text{ M}^{-1} \text{ s}^{-1}$ for TEOA, demonstrating that the reductive quenching depends on TEOA (Figure S5 in the Supporting Information). The quenching of EY^{2-*} with TEOA was also reported by observing the transient absorption spectra by laser photolysis.³⁸

In addition, other organic chromophores (rose bengal and phloxine B) that have been often used as visible-light photosensitizers in other photoreactions were also investigated and compared to eosin (Table S1 in the Supporting Information; the chemical structures of the chromophores are also shown). Photogeneration of NADH was found to occur when each of these photosensitizers was used in place of eosin but at significantly lower levels.

Because other sacrificial electron donors have often been used for photocatalytic reduction reactions, ethylenediaminetetraacetic acid, sodium formate, and triethylamine were studied instead of TEOA. These compounds resulted in only trace amounts of NADH production under the same reaction conditions at pH 7.0. TEOA was also found to be the most effective among the compounds at H_2 photoproduction using cobalt molecular catalysts.²³

Finally, in order to couple the **1**/eosin Y/ NAD^+ /TEOA system with NADH-dependent enzymes, the conversion of CO_2 to formic acid was performed using FDH (Scheme 1).

Scheme 1. Conversion of CO_2 to Formic Acid by FDH and NADH



After 4 h of illumination, formic acid (0.14 mM) was observed (Figure 7), demonstrating that the enzyme utilized NADH

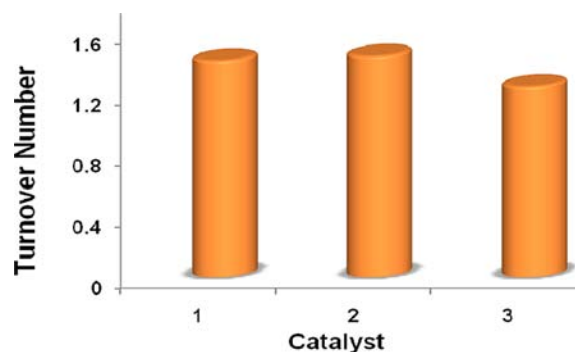
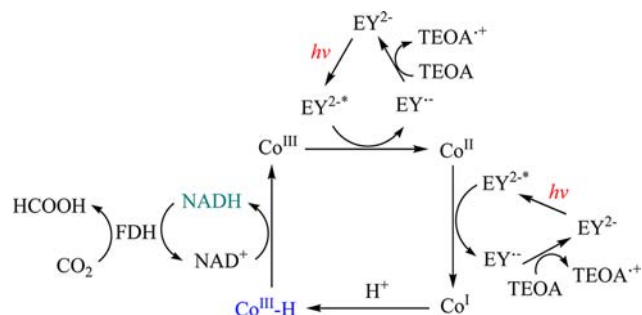


Figure 7. Turnover numbers for the conversion of CO_2 to formic acid. The numbers correspond to turnovers of eosin. Reaction conditions: 0.13 mM **1**–**3**, 0.10 mM eosin Y, 0.50 mM NAD^+ , 0.20 M TEOA, and 5 units of FDH in 0.15 M phosphate buffer (pH 7.0) upon 4 h of irradiation at 25 °C.

generated during the photochemical process. The conversion yield to formic acid corresponded to 1.5 turnovers of eosin (1.2 turnovers of NAD^+) in the photoproduction system of **1**/eosin/TEOA. These data demonstrate that NAD^+ was regenerated during the photoproduction of NADH by **1** and consumption by FDH. Even upon irradiation for 9 h, the conversion yield for CO_2 was not significantly improved. The activity of FDH or immobilized FDH for CO_2 conversion was determined to be over 95% based on the initial amount of NADH.³⁹ The catalysts **2** and **3** also produced formic acid, but a low yield was obtained using **3** relative to the amount of NADH photochemically generated under the same conditions.

On the basis of all of the observations described above, we propose a mechanism for visible-light-driven reduction of NAD^+ using cobaloxime and eosin in the presence of TEOA (Scheme 2). The photoexcited eosin probably reduced the starting cobalt(III) species to a cobalt(II) intermediate and then to cobalt(I). Photochemical and electrochemical formation of such cobalt(I) species was also reported with the same and similar cobalt complexes.^{20,21,24,25} The cobalt(I) species is then protonated to generate a cobalt(III) hydride intermediate. Another possibility that could occur before hydride transfer to NAD^+ is cobalt(III) hydride may be further

Scheme 2. Proposed Overall Cycles for Photocatalytic NADH Production with Cobalt Catalyst/Eosin Y/TEOA and Successive CO₂ Reduction with FDH^a



^aPossible H₂ production steps were omitted for simplicity.

reduced to produce a cobalt(II) hydride species. Similar mechanisms suggesting involvement of the cobalt(III) and cobalt(II) hydride species were proposed for the photo-production of H₂.^{17–21,24,25} Finally, the cobalt(III) hydride species may transfer its hydride to generate NADH. The TEOA radical species (TEOA^{•+}), which is produced after reducing the radical eosin (EY^{•-}), loses H⁺ and transfers a second electron during its decomposition path to glycolaldehyde and di-(ethanol)amine, which has been proposed in other photochemical studies.^{40,41} NADH generated in the photoreactions with 1–3 was utilized to reduce CO₂ to formic acid in the presence of FDH. The results of this study provide insight into mechanisms of photocatalytic NADH production with the molecular cobalt catalysts and subsequent CO₂ reduction with FDH.

CONCLUSIONS

A visible-light-driven photosystem containing the cobalt(III) bis(dimethylglyoximate) catalyst, an organic chromophore, and a sacrificial electron donor has been developed to produce the enzymatically active NADH. The results of this study provide insight into the mechanism of photocatalytic NADH production with a low-transition-metal complex. The NADH production rate was dependent on the cobalt catalyst, NAD⁺, and TEOA. These results suggest that electron transfer from EY^{2-*} to the cobalt center to generate the cobalt hydride species is the important step in catalytic NADH generation. The catalytic cycle in this photoreaction system was directly connected to the conversion of CO₂ to formic acid using FDH. These findings demonstrate that the first earth-abundant cobalt catalyst was able to reduce NAD⁺ in aqueous solution and the photoreaction system was also coupled with FDH to reduce CO₂. Further studies are in progress to modify the ligand environment of the cobalt complex for more efficient NADH regeneration and maximize the coupling between two catalytic systems, such as NADH photoproduction and CO₂ conversion.

ASSOCIATED CONTENT

Supporting Information

Photoproduction yield of NADH, representative absorption spectral changes in NADH formation, visible-light-driven NADH production, UV–vis absorption spectra, time dependence of NADH production, and emission spectra of eosin. This material is available free of charge via the Internet at <http://pubs.acs.org>.

AUTHOR INFORMATION

Corresponding Author

*E-mail: jinheung@ewha.ac.kr. Phone: +82-2-3277-4453. Fax: +82-2-3277-3419.

Notes

The authors declare no competing financial interest.

ACKNOWLEDGMENTS

This work was supported by the KRICT-2020 Program, the Ewha Global Top5 Grant 2011 of Ewha Womans University, and BK21 (to J.A.K., S.K., and J.L.).

REFERENCES

- Hambourger, M.; Gervaldo, M.; Svedruzic, D.; King, P. W.; Gust, D.; Ghirardi, M.; Moore, A. L.; Moore, T. A. *J. Am. Chem. Soc.* **2008**, *130*, 2015.
- Kotani, H.; Hanazaki, R.; Ohkubo, K.; Yamada, Y.; Fukuzumi, S. *Chem.—Eur. J.* **2011**, *17*, 2777.
- Miyatani, R.; Amao, Y. *Biotechnol. Lett.* **2002**, *24*, 1931.
- Itoh, T.; Asada, H.; Tobioka, K.; Kodera, Y.; Matsushima, A.; Hiroto, M.; Nishimura, H.; Kamachi, T.; Okura, I.; Inada, Y. *Bioconjugate Chem.* **2000**, *11*, 8.
- Andreesen, J. R.; Ghazzawi, E. E.; Gottschalk, G. *Arch. Microbiol.* **1974**, *96*, 103.
- Mertens, R.; Greiner, L.; van den Ban, E. C. D.; Haaker, H. B. C. M.; Liese, A. *J. Mol. Catal. B: Enzym.* **2003**, *24–25*, 39.
- Groger, H.; Hummel, W.; Buchholz, S.; Drauz, K. H.; van Nguyen, T.; Rollmann, C.; Husken, H.; Abokitse, K. *Org. Lett.* **2003**, *5*, 173.
- Lutz, J.; Mozhaev, V. V.; Khmelnitsky, Y. L.; Witholt, B.; Schmid, A. *J. Mol. Catal. B: Enzym.* **2002**, *19–20*, 177.
- Schmid, A.; Vereyken, I.; Held, M.; Witholt, B. *J. Mol. Catal. B: Enzym.* **2001**, *11*, 455.
- Ruppert, R.; Herrmann, S.; Steckhan, E. *Tetrahedron Lett.* **1987**, *6583*.
- Ruppert, R.; Herrmann, S.; Steckhan, E. *J. Chem. Soc., Chem. Commun.* **1988**, 1150.
- Steckhan, E.; Herrmann, S.; Ruppert, R.; Dietz, E.; Frede, M.; Spika, E. *Organometallics* **1991**, 1568.
- Wienkamp, R.; Steckhan, E. *Angew. Chem., Int. Ed. Engl.* **1983**, *22*, 497.
- Maenaka, Y.; Suenobu, T.; Fukujumi, S. *J. Am. Chem. Soc.* **2012**, *134*, 367.
- Maenaka, Y.; Suenobu, T.; Fukujumi, S. *J. Am. Chem. Soc.* **2012**, *134*, 9417.
- Connolly, P.; Espenson, J. H. *Inorg. Chem.* **1986**, *25*, 2684.
- Hu, X.; Brunschwig, B. S.; Peters, J. C. *J. Am. Chem. Soc.* **2007**, *129*, 8988.
- Hu, X.; Cossairt, B. M.; Brunschwig, B. S.; Lewis, N. S.; Peters, J. C. *Chem. Commun.* **2005**, 4723.
- Berben, L. A.; Peters, J. C. *Chem. Commun.* **2010**, 398.
- Dempsey, J. L.; Winkler, J. R.; Gray, H. B. *J. Am. Chem. Soc.* **2010**, *132*, 16774.
- Razavet, M.; Artero, V.; Fontecave, M. *Inorg. Chem.* **2005**, *44*, 4786.
- Baffert, C.; Artero, V.; Fontecave, M. *Inorg. Chem.* **2007**, *44*, 1817.
- Lazarides, T.; McCormick, T.; Du, P.; Luo, G.; Lindley, B.; Eisenberg, R. *J. Am. Chem. Soc.* **2009**, *131*, 9192.
- Du, P.; Knowles, K.; Eisenberg, R. *J. Am. Chem. Soc.* **2008**, *130*, 12576.
- Du, P.; Schneider, J.; Luo, G.; Brennessel, W. W.; Eisenberg, R. *Inorg. Chem.* **2009**, *48*, 4952.
- McCormick, T. M.; Calitree, B. D.; Orchard, A.; Kraut, N. D.; Bright, F. V.; Detty, M. R.; Eisenberg, R. *J. Am. Chem. Soc.* **2010**, *132*, 15480.

- (27) McCormick, T. M.; Han, Z.; Weinberg, D. J.; Brennessel, W. W.; Holland, P. L.; Eisenberg, R. *Inorg. Chem.* **2011**, *50*, 10660.
- (28) Sun, Y.; Bigi, J. P.; Piro, N. A.; Tang, M. L.; Long, J. R.; Chang, C. J. *J. Am. Chem. Soc.* **2011**, *133*, 9212.
- (29) Bhoware, S. S.; Kim, K. Y.; Kim, J. A.; Wu, Q.; Kim, J. J. *Phys. Chem. C* **2011**, *115*, 2553.
- (30) Schrauzer, G. N. *Inorg. Synth.* **1968**, *11*, 61.
- (31) Hollmann, F.; Witholt, B.; Schmid, A. J. *Mol. Catal. B: Enzym.* **2003**, *19–20*, 167.
- (32) Hollmann, F.; Schmid, A.; Steckhan, E. *Angew. Chem., Int. Ed.* **2001**, *40*, 169.
- (33) Hoehn, S. T.; Junker, H.-D.; Bunt, R. C.; Turner, C. J.; Stubbe, J. *Biochemistry* **2001**, *40*, 5894.
- (34) Rajani, C.; Kincaid, J. R.; Petering, D. H. *J. Am. Chem. Soc.* **2004**, *126*, 3829.
- (35) Stewart, R. *Oxidation Mechanisms*; Benjamin: New York, 1964.
- (36) Tung, H. C.; Sawyer, D. T. *J. Am. Chem. Soc.* **1992**, *114*, 3445.
- (37) Probst, B.; Kolano, C.; Hamm, P.; Alberto, R. *Inorg. Chem.* **2009**, *48*, 1836.
- (38) Islam, S. D.-M.; Konishi, T.; Fujitsuka, M.; Ito, O.; Nakamura, Y.; Usui, Y. *Photochem. Photobiol.* **2000**, *71*, 675.
- (39) Lu, Y.; Jiang, Z.; Xu, S.; Wu, H. *Catal. Today* **2006**, *115*, 263.
- (40) Kalyanasundaram, K.; Kiwi, J.; Grätzel, M. *Helv. Chim. Acta* **1978**, *61*, 2720.
- (41) Du, P.; Schneider, J.; Jarosz, P.; Eisenberg, R. *J. Am. Chem. Soc.* **2006**, *128*, 7726.